TECHNICAL TRANSACTIONS | CZASOPISMO TECHNICZNE
ELECTRICAL ENGINEERING | ELEKTROTECHNIKA
1-E/2015

PIOTR MYNAREK, MARCIN KOWOL*

THERMAL ANALYSIS OF A PMSM USING FEA AND LUMPED PARAMETER MODELING

ANALIZA CIEPLNA SILNIKA PMSM ZA POMOCĄ METODY ELEMENTÓW SKOŃCZONYCH ORAZ SCHEMATU CIEPLNEGO

Abstract

Permanent magnet synchronous motors are often used in hybrid electric vehicles due to the high power density. Overheating in a PMSM motor can cause negative effects on the work of permanent magnets and a significant shortening of the life of the machine due to the phenomenon of the thermal ageing of insulation. Therefore, it is extremely important to know the exact temperature distribution in different parts of the electrical machine under various operating conditions. This paper presents a lumped parameter thermal model and FE model of a permanent magnet synchronous motor. A method for the homogenization of a stator winding is also described. In order to validate the accuracy of the calculation results, measurements on the physical model of the machine were carried out.

Keywords: *PMSM*, *thermal analysis*, *homogenization*

Streszczenie

Silniki synchroniczne z magnesami trwałymi dzięki dużej gęstości mocy są coraz chętniej wykorzystywane w różnych gałęziach przemysłu. Zbyt duże nagrzewanie silnika PMSM może wpływać negatywnie na pracę magnesów trwałych oraz spowodować skrócenie czasu życia maszyny w wyniku termicznego starzenia się izolacji. Dlatego też niezmiernie ważna jest dokładna znajomość rozkładu temperatury w poszczególnych częściach maszyny elektrycznej, w różnych jej stanach pracy. W artykule przedstawiono analizę cieplną silnika synchronicznego z magnesami trwałymi przeprowadzoną metodą schematów cieplnych, jak również metodą elementów skończonych (MES). Opisano także metodę homogenizacji uzwojeń wsypywanych. Wyniki symulacji komputerowych zostały zweryfikowane pomiarowo na obiekcie rzeczywistym silnika.

Słowa kluczowe: *silnik PMSM*, *analiza cieplna*, *homogenizacja*

DOI: 10.4467/2353737XCT.15.031.3831

* Ph.D. Eng. Piotr Mynarek, Ph.D. Eng. Marcin Kowol, Faculty of Electrical Engineering, Automatic Control and Informatics, Opole University of Technology.

1. Introduction

New constructional solutions applied by aircraft and automotive industries use electric motors more and more often. Such solutions allow more energy efficient processing and the reduction of emissions. One of the major factors when selecting the most appropriate electric motor for the propulsion system is the power density, therefore, permanent magnet synchronous motors are increasingly being used [3]. Rotor design solutions give the possibility to develop the highest possible density torque in a relatively small volume. In addition, PMSM are characterized by high efficiency and a wide range of power at constant rotational speed.

Placing an electric motor, for example in a compartment in a vehicle, causes significant deterioration of cooling conditions. Therefore, an accurate knowledge of the temperature distribution in different parts of the electric motor during its various operating conditions is an extremely important issue. Thermal analysis of electric motors primarily uses the lumped parameter thermal models [3, 4] and the finite elements method (FEM) [1, 6]. This paper presents a permanent magnet synchronous motor based on both calculation methods. The application of both methods enables an effective analysis of the machine.

2. Determination of power losses

The research subject of the study is SMKwsg90M8 motor with the start-up frequency and parameters presented in Table 1.

Table 1

Selected parameters of the machine

Physical size	U_n [V]	I_n [A]	P_n [kW]	n_n [rev/obr]	η [%]
Value	400	3.7	2	2200	91

During the first stage of the research work, power losses in the analysed motor were determined. For this purpose, a numerical model was built, which, together with the discretization mesh, is shown in Fig. 1. During the building of the field model of the analysed motor, periodic boundary conditions were applied, thus limiting the calculation area to one fourth of the volume of the entire machine. This procedure allowed a significant reduction in the computation cost needed to solve the problem.

The main sources of heating in synchronous machines come from the heating effect according to Joule's law and core losses. Omitting the skin and proximity effects, losses occurring in the windings can be determined in accordance with the formula:

$$\Delta P_{cu} = RI^2 \tag{1}$$

where:
R – the phase resistance,
I – the phase current.

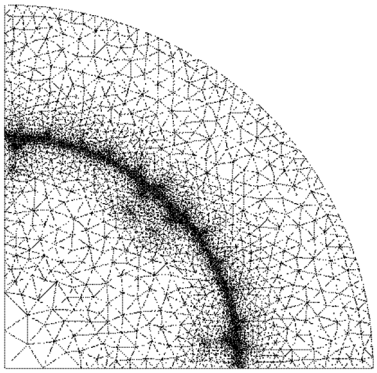

Fig. 1. Discretization mesh in cross-section of the motor

The second major thermal source in electric motors comes from iron losses ΔP_{Fe}. Due to the fact that the object of the research study is a synchronous motor, the losses are mainly formed in the stator. Losses in the rotor are smaller and caused by higher harmonics of magnetic flux density. Iron losses were estimated by using Bertotti's formula considering the losses from the hysteresis loop, eddy current and excess losses [6]. Coefficients of hysteresis and excess losses have been estimated on the basis of electrical steel sheet losses given in the manufacturer's specifications.

$$\Delta P_{Fe} = \iiint_V (k_h B_m^2 f\, k_f + \frac{1}{T}\int_0^T \left[\sigma \frac{d^2}{12}\left(\frac{\mathrm{d}B}{\mathrm{d}t}(t)\right)^2 + k_e \left(\frac{\mathrm{d}B}{\mathrm{d}t}(t)\right)^{\frac{3}{2}} \right] k_f \mathrm{d}t)\mathrm{d}V \tag{2}$$

where:
k_h – the hysteresis coefficient,
B_m – maximum flux density excursion over an electrical cycle,
f – the frequency,
k_f – the packing factor of the laminated core pack,
σ – the electric conductivity,
d – the thickness of a single sheet of lamination,
k_e – the excess loss coefficient,
V – the volume of the region.

Using formula (2), losses ΔP_{Fe} are calculated in each element of the discretisation mesh being formed in the 2D model for a particular region, and then averaged across the volume of the region. Losses were determined for three characteristic areas of the machine, specifically, the yoke, stator teeth and rotor. Table 2 lists power losses for the selected working state of the analyzed machine.

Table 2

Calculated loss in PMSM

Load on the motor ($n = n_N$)	Losses ΔP_{Cu} [W]	Losses ΔP_{Fe} [W]		
		Stator teeth	Stator yoke	Rotor
$T_l = 8.70$ Nm	64.89	40.6	21.8	11.6

3. Estimation of the heat transfer coefficient

One of the major problems in thermal analysis is the proper consideration of heat transfer intensity in the analyzed object. The most convenient method of considering this is to apply Newton's boundary condition. The application of Newton's boundary condition of cooling directly allows considering the intensity of cooling in the form of heat transfer coefficient α. However, the correctly calculating the coefficient gives rise to many problems. Therefore, this study proposes the estimation of the heat transfer coefficient based on calibration measurements. This approach enables determining the searched value for the specific motor housing in every typical point, that is for a motor housing fin and for gaps between the fins. Furthermore, it is possible to determine the dependence between α coefficient and the motor rotational speed, rather than the coolant velocity. It is undoubtedly more practical and intuitive when performing thermal analysis for a particular state of the machine.

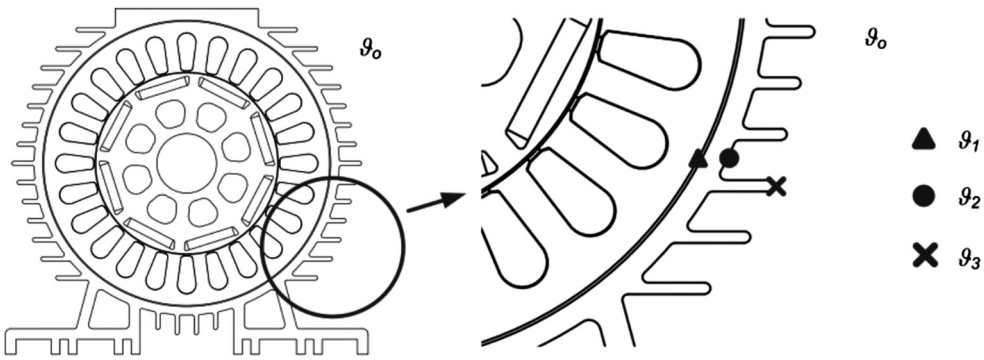

Fig. 2. Cross-section of motor along with marked measuring points, where: ϑ_1 – temperature between stator and motor housing; ϑ_2 – motor housing temperature between cooling fins; ϑ_3 – fin temperature; ϑ_o – ambient temperature

According to Newton's condition of heating, the heat flux q being transferred in a solid object equals the flux being transferred to the ambient.

$$q_\alpha = \lambda \left.\frac{\partial \vartheta}{\partial n}\right|_F = \alpha\left(\vartheta_F - \vartheta_o\right) \tag{3}$$

By measuring the temperature at the points shown in Fig. 2, it is possible to designate coefficient α with satisfactory accuracy. Based on temperatures ϑ_1 and ϑ_2 (ϑ_3), as well as when the exact dimensions of the housing are known, the heat transferred within the solid object can be determined. Considering the heat flux, surface and ambient temperatures, by using the equation (3), the heat transfer coefficient for the motor housing between cooling fins (4), although separately – just for the cooling fins (5) can be determined.

$$\alpha_o = \frac{\vartheta_1 - \vartheta_2}{\left(\frac{d_1}{\lambda_1} + \frac{d_2}{\lambda_2}\right)\left(\vartheta_2 - \vartheta_o\right)} \tag{4}$$

where:
d_1, d_2 – air layer thickness (of housing),
λ_1, λ_2 – coefficient of the air thermal conductivity (aluminum).

$$\alpha_z = \frac{\vartheta_1 - \vartheta_3}{\left(\frac{d_1}{\lambda_1} + \frac{d_2'}{\lambda_2}\right)\left(\vartheta_3 - \vartheta_o\right)} \tag{5}$$

where: d'_2 – housing layer thickness together with the high typical for the cooling fin.

On the basis of the performed measurements, the heat transfer coefficients were determined at both typical points on the motor housing as a function of the rotational speed. Figure 3 indicates measurement results and an approximate relationship of the α coefficient as a function of motor rotational speed.

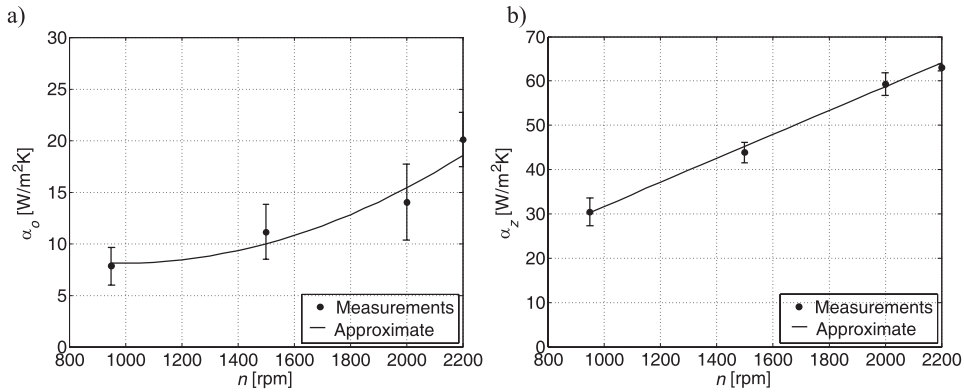

Fig. 3. Dependency of heat transfer coefficient for a housing between cooling fins (a) and for a single cooling fin (b) as a function of motor rotational speed

4. Homogenization of windings

In terms of heating, a sensitive area in permanent magnet synchronous motors is the stator winding as the highest temperature occurs here. Proper modeling of the windings, in particular windings with randomly wound insulated coil, causes many problems because of the high complexity of the object's structure [5]. In order to determine thermal conductivity of the impregnated winding (λ_{iw}) for the analysed motor, it was decided to design two coils: one impregnated and one non-impregnated, both placed in a segment of the stator (Fig. 4a). Coil winding data and stator segment dimensions correspond to the technical data of the analyzed machine. In both coils, five K-type thermocouples ($T1$–$T5$) were placed along the height of the slots (Fig. 4b).

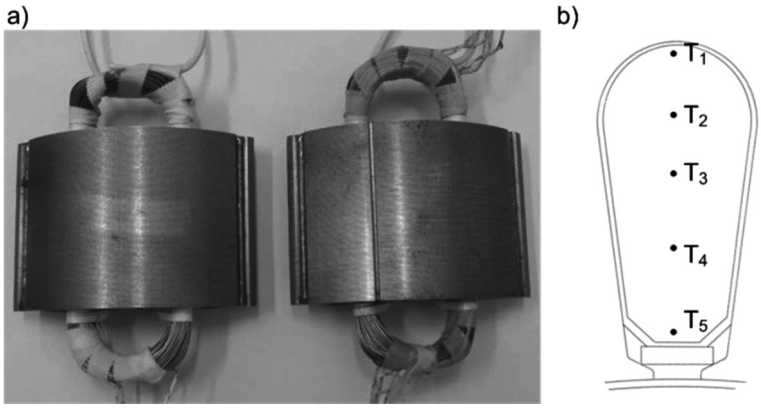

Fig. 4. Constructed coils (a) and arrangement of the thermocouples in the coil (b)

Figure 5 shows schematic diagram of the proposed method for determining the thermal conductivity of an impregnated winding.

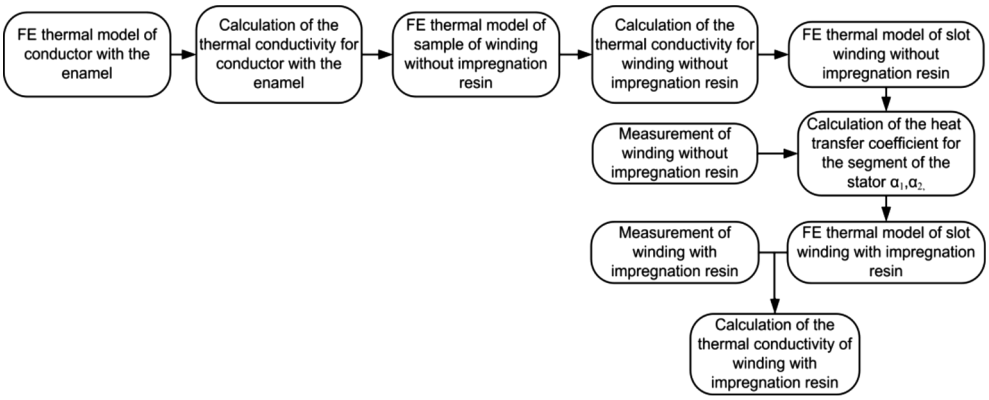

Fig. 5. The proposed method for determining the thermal conductivity of impregnated windings

In order to determine the equivalent thermal conductivity of conductors with enamel, the formula presented below was used:

$$\lambda_{ec} = \left(\frac{d' - \delta_e}{2\delta_e} \right) \lambda_e \tag{6}$$

where:
d' – diameter of the conductor with enamel,
δ_e – thickness of the enamel layer,
λ_e – thermal conductivity of enamel.

The thermal conductivity of non-impregnated winding $\lambda_{ni\,w}$ = 0.1 W/(mK), along the *OX* axis as well as the *OY* axis. This coefficient was calculated based on the numerical model of the winding sample with filling coefficient similar to the one, as in the case of the real winding – k = 51% (Fig. 6) and adapted in the Fourier's law (7) [1].

$$\lambda_{ni\,w\,x} = \frac{q_x \cdot d}{\vartheta_1 - \vartheta_2} \tag{7}$$

where:
q_x – heat flux transferred across the wall,
l – the thickness of the wall,
ϑ_1, ϑ_2 – the temperatures of the walls,
$\lambda_{ni\,w\,x}$ – thermal conductivity of the non-impregnated winding in the x-axis direction.

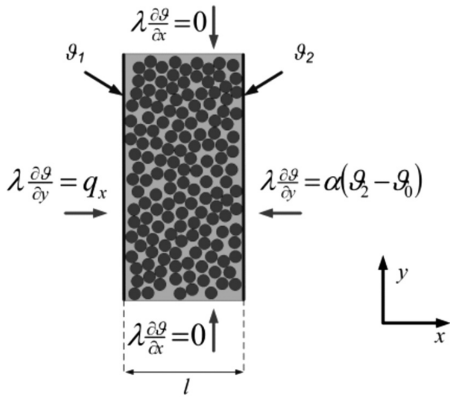

Fig. 6. FE model of the winding sample

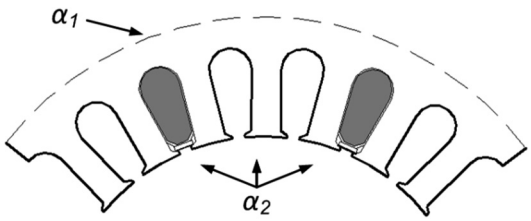

Fig. 7. The values of the coefficient of heat transfer for stator segment

As the values of power losses occurring in the non-impregnated coil and the thermal conductivity were known, the heat transfer coefficient α for the segment of the core was estimated. For the analysed measuring object of the outer layer of the core, the estimated coefficient α is α_1 = 10 W/(m^{2}K), while for the other layers, it is α_2 = 6 W/(m^{2}K) (Fig. 8).

While maintaining the same measurement conditions for both coils, it is possible to also adopt the designated heat transfer coefficients for the impregnated coil. Then, based on the field model of the impregnated coil and measurement results, the impregnated winding thermal conductivity coefficient λ_{iw}, was estimated, for which the value is λ_{iw} = 0.18 W/(mK).

5. Lumped parameter thermal model of PMSM

The mathematical model, by which the transient thermal analysis of the analysed PMSM was carried out, was built on the basis of a lumped parameter thermal method. In this model, the following assumptions were adopted: the machine is symmetrical; mechanical losses are omitted; the thermal transfer coefficient is averaged in respect to the entire machine housing surface.

Particular heat transfer paths between respective elements of the analysed machine have assigned corresponding thermal resistance. The thermal resistance for heat transfer in the conductivity state was determined based on the formula [7]:

$$R_{th} = \frac{h}{\lambda S} \tag{8}$$

where:
h – active length that is parallel to the heat flux,
λ – thermal conductivity,
S – cross-sectional area that is normal to the heat flux.

While the thermal resistance value for convection phenomena was based on the following formula:

$$R_{th} = \frac{1}{\alpha S_c} \tag{9}$$

where:
α – convective heat transfer coefficient,
S_c – heat transfer surface area.

The model considers the thermal capacity of the motor's individual components, which was computed from:

$$C_{th} = c_w \rho V \tag{10}$$

where:
c_w – specific heat capacity,
ρ – density,
V – volume.

A PMSM mathematical model in the form of a thermal circuit was implemented in PLECS software (Fig. 8).

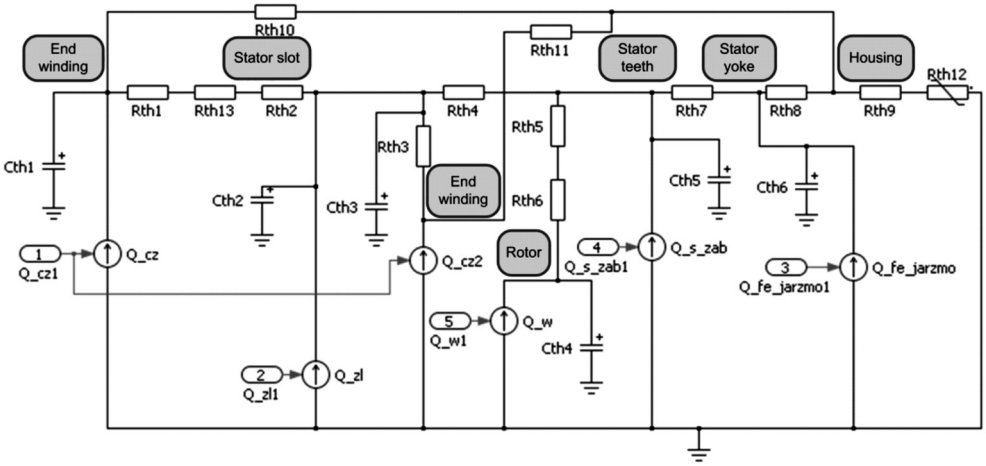

Fig. 8. Thermal model of the analysed motor in PLECS toolbox

By using the thermal circuit, a number of computer simulations for different PMSM operating states were performed. The results obtained are verified by measurements performed on the real object of the motor. For this purpose, a measuring stand was built based on the authors' data acquisition system – this is described in detail in [2]. Figures 9 and 10 show temperature changes at selected measuring points, for nominal motor operating conditions.

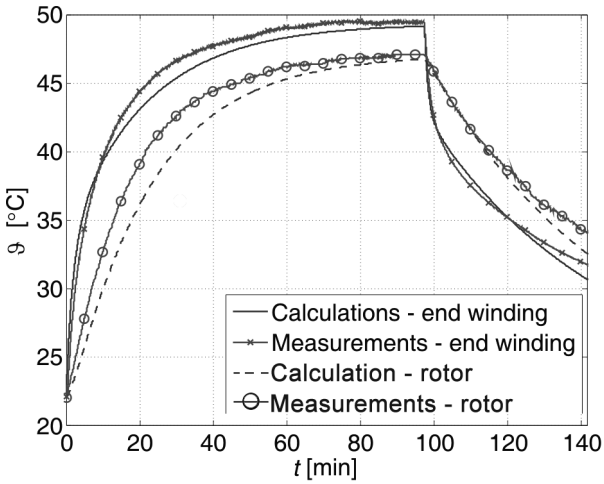

Fig. 9. Temperature change in the end winding and in the rotor (heating and cooling process)

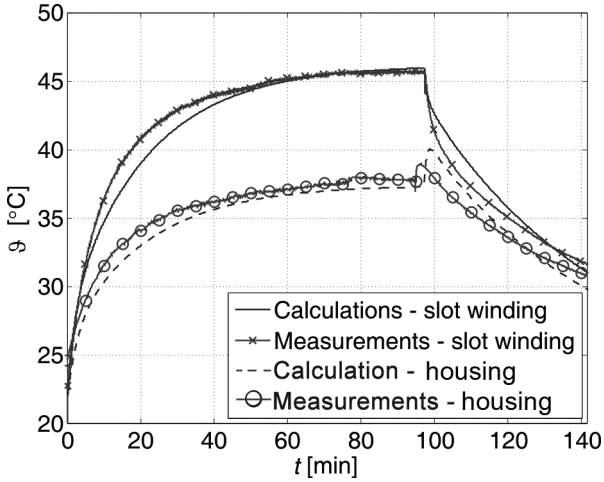

Fig. 10. Temperature change in winding slots and on the motor housing (heating and cooling process)

6. Thermal calculations of PMSM by using field model

The stage of the research study on the analysed motor, thermal analysis in steady state was carried out. For this purpose, a two-dimensional field model was built. During the construction process of the analysed motor field model, symmetry conditions were applied, thus limiting the calculation area to one-eighth of the machine's entire volume, which allowed reducing the numerical costs. The model adopts similar simplifying assumptions to the thermal circuit model. The further adopted value of the heat transfer coefficient was adjusted by the surface heat transfer coefficient and thermal resistance of the housing, which allowed omission of the motor housing parameter.

Table 3 lists computer simulation results carried out on the developed two mathematical models with measurement results performed on the real object of the motor.

Table 3

The results of calculations and measurements

Measuring point	Calculations lumped parameter models ϑ_{LP} [°C]	Calculations MES ϑ_{MES} [°C]	Measurement ϑ_m [°C]
End-winding	48.6	–	49.4
Stator slot	46.8	47.1	45.6
Rotor	46.1	46.5	47.1
Housing	36.9	38.7	38.4

7. Conclusions

This paper has presented permanent magnet synchronous thermal. Satisfactory convergence with measurements performed on the actual physical motor was obtained. The presented thermal modeling operating method of the analysed motor combines advantages of field models and lumped parameter models. The lumped element models allow obtaining temperature increments in particular parts of the machine at relatively low numerical costs. However, it should be noted that determining a thermal equivalent circuit and thermal parameters is a relatively difficult task, especially for windings. On the other hand, field models allow obtaining accurate temperature distribution in the machine, which enables determining local high temperature spots.

References

[1] Idoughi L., Mininger X., Bouillault F., Bernard L., Hoang E., *Thermal Model with Winding Homogenization and FIT Discretization for Stator Slot*, IEEE Transactions on Magnetics, December 2011, Vol. 47, No. 12, pp. 4822–4826.

[2] Kowol M., Mynarek P., Kołodziej J., *Application of LabVIEW environment for permanent magnet synchronous motor testing*, Poznan University of Technology, Academic Journals, Electrical Enginnering, Computer Applications in Electrical Enginnering, Issue 75, Poznań 2013, pp. 49–56.

[3] Lee B., Kim K., Jung J., Hong J., Kim Y., *Temperature Estimation of IPMSM Using Thermal Equivalent Circuit*, IEEE Transactions on Magnetics, November 2012, Vol. 48, No. 11, pp. 2949–2952.

[4] Nategh S., Wallmark, O., Leksell M., Zhao S., *Thermal Analysis of a PMaSRM Using Partial FEA and Lumped Parameter Modeling*, IEEE Transactions on Energy Conversion, June 2012, Vol. 27, No. 2, pp. 477–488.

[5] Simpson N., Wrobel R., Mellor P.H., *Estimation of Equivalent Thermal Parameters of Impregnated Electrical Windings*, IEEE Transactions on Industry Applications, Nov.–Dec. 2013, Vol. 49, No. 6, pp. 2505–2515.

[6] Wrobel R., Mellor P.H., McNeill N., Staton D.A., *Thermal Performance of an Open--Slot Modular-Wound Machine with External Rotor*, IEEE Transactions on Energy Conversion, 2010, Vol. 25, No. 2, pp. 403–411.

[7] Wrobel R., Mellor P.H., *Thermal Design of High-Energy-Density Wound Components*, IEEE Transactions on Industrial Electronics, September 2011, Vol. 58, No. 9, pp. 4096–4104.